การจำกัดในการไหลสวนกันในท่อราบซึ่งต่อกับท่อโค้ง, ตอนที่ 2:ทฤษฎี

COUNTERCURRENT FLOODING IN A HORIZONTAL PIPE WITH BEND, PART II : THEORY

สมชาย วงศ์วิเศษ

Somchai Wongwises

ศูนย์วิจัยกลศาสตร์ของไหลและเครื่องจักรเทอร์โบ

ภาควิชาวิศวกรรมเครื่องกล คณะวิศวกรรมศาสตร์

สถาบันเทคโนโลยีพระจอมเกล้าธนบุรี

Fluid & Turbomachinery Research Centre (FUTURE)

Department of Mechanical Engineering

Faculty of Engineering

King Mongkut's Institute of Technology Thonburi

บทคัดย่อ

แบบจำลองทางคณิตศาสตร์ได้รับการพัฒนาเพื่อทำนายจุดเริ่มต้นของฟลัดดิ้งสำหรับท่อราบซึ่งต่อกับท่อโค้ง การวิเคราะห์ทำได้โดยการพิจารณาในส่วนของท่อราบซึ่งเป็นการไหลแบบแยกชั้นที่มีผิวหน้าราบเรียบ ประกอบกับสมการที่ได้มาจากการทดลองซึ่งเป็นความสัมพันธ์ของพารามิเตอร์ขณะเกิดสลักกิ้งในบริเวณใกล้ส่วนโค้ง ผลการคำนวณได้ถูกเปรียบเทียบกับผลที่ได้จากการทดลอง รวมทั้งเปรียบ-เทียบกับผลการทดลองจากนักวิจัยอื่น ๆ และพบว่าการทำนายโดยใช้แบบจำลองที่เสนอนี้ให้ผลที่สมเหตุสมผล โดยเฉพาะเมื่อพิจารณาในแง่ของความยาวต่อเส้นผ่าศูนย์กลางของท่อที่ใช้

ABSTRACT

A mathematical model is developed to predict the onset of flooding in a horizontal pipe with bend. The model is based on an analysis of smooth horizontal stratified flow together with an empirical correlation for the onset of slugging at the hydraulic jump which is formed just downstream of the bend. Flooding curves calculated by this model are compared with own experimental data and those of other researchers. The predictions of the onset of flooding are in reasonable agreement especially when the length to diameter ratio of the pipe is concerned.

Keywords: onset of flooding, slugging, stratified flow, supercritical flow, hydraulic jump, void fraction

INTRODUCTION

The experimental results described in part I [14] clearly demonstrate that flooding in a pipe with bend is a complicated phenomenon despite some similarities observed in vertical and horizontal flooding. Quantitatively, flooding in this kind of pipe geometry occurs at gas flows much smaller than those needed to produce flooding in a vertical pipe of equal diameter. This difference is due to the wave instability that causes flooding in the horizontal pipe. Bankoff et al. [1] have discussed five theoretical models of slug formation in cocurrent horizontal flow and show that the models can be applied to countercurrent flow. Taitel et al. [2] proposed that the transition from stratified to intermittent flow occurs as result of instability of a solitary wave on a horizontal stratified liquid layer. This is somewhat similar to phenomena observed in the case of the hydraulic jump in a horizontal pipe with bend [3]. Ardron et al. [4] presented a model based on the instablility of the gas/liquid interface and the formation of a hydraulic jump in the horizontal pipe.

CALCULATION OF FLOODING CURVES

In order to compare with the experimental results, the theoretical flooding curves will be derived to show the curves in form of the gas and liquid velocity. The flow phenomena which is observed from the experiment and used as a basis for the calculation is shown in *Figure 1.* A horizontal pipe is connected with an inclined pipe by a bend. Liquid is injected at A through the liquid inlet section at a constant flow rate and flows down the wall of inclined pipe and then along the bottom of the horizontal pipe in stratified flow to the liquid outlet section. Gas is injected into the system at E and flows countercurrently to liquid flow. The critical conditions for flooding for this kind of pipe geometries are those at C and the interaction between the inclined and horizontal pipe is vital for understanding the phenomena. The flow of liquid from the inclined pipe is initially supercritical at B. The transition of the flow to subcritical flow occurs near the bend at the horizontal section. This transition form a hydraulic jump at C which is the point of maximum liquid depth. The level of liquid in the horizontal pipe decreases continuously to the direction of liquid outlet (E) at which the

liquid level is minimum. Because the cross-sectional area of flow is changed, the liquid velocity increases continuously until it becomes critical at the liquid inlet section.

The described flooding conditions can be solved by using the mass and momentum conservation for steady stratified two-fluid flow [4] between the hydraulic jump and the liquid outlet. Neglecting viscous interactions and for the ignoring pressure changes at the interface due to surface tension, the one-dimensional equations for mass and momentum conservation for phase k (k: L=Liquid, G=Gas) for the steady horizontal stratified flow of two incompressible fluids can be written as

$$\frac{\partial(\varepsilon_k \bar{v}_k)}{\partial \chi} = 0, \tag{1}$$

$$\varepsilon_k \rho_k \bar{v}_k \frac{\partial \bar{v}_k}{\partial \chi} + \varepsilon_k \frac{\partial \bar{P}_k}{\partial \chi} - (P_i - \bar{P}_k)$$

$$\frac{\partial \varepsilon_k}{\partial \chi} = -\tau^*_{wk} - \tau^*_{ik}, \tag{2}$$

where $\bar{V}_k$ is average velocity of phase k, ε_L is liquid hold-up and ε_G is void fraction, x is the distance from point C, $\bar{P}_k$ is the pressure in bulk phase k and p_i is the pressure on the interface, $\tau^*_{w\kappa}$ and $\tau^{*i}_{i\kappa}$ are wall shear force and interfacial shear force per unit flow volume acting on phase k and are defined by

$$\tau^*_{wG} = -\left|\tau_{wG}\right| \frac{\xi_{wG}}{F}$$
$$\tau^*_{wL} = \left|\tau_{wL}\right| \frac{\xi_{wL}}{F} \tag{3}$$
$$\tau^*_{iG} = -\tau_{iL} = -\tau_i \frac{\xi_i}{F}$$

Where ξ represents the perimeters which can be expressed in terms of the angle, β *(Figure 2).*

$\xi_{wG} = (\pi-\beta/2)\,D$, $\xi_{wL} = \beta D/2$, $\xi_i = D\sin(\beta/2)$,

$$\varepsilon_L = \frac{1}{2\pi}\left(\beta - \frac{2}{\pi}\sin(\beta)\right) \tag{4}$$

If the pressure variation over the cross section of each phase is due to hydrostatic forces only;

$$\bar{P}_k = P_i + \rho_k g(y_i - \bar{y}_k) \tag{5}$$

where y_i is the elevation of the interface, and $\bar{y}_k$ is the elevation of the centroid of F_k, both with respect to an arbitrary datum. The overbars shows the phase-average quantities, defined by

$$\bar{f}_k = \frac{1}{F_k}\int_{F_k} f_k \, dF \tag{6}$$

where F_k is the portion of pipe which is occupied by Phase k. Substitution the parameters in Eqs. (3), (4), (5) into Eq. (2), the momentum equation of each phase will be modified to

$$\varepsilon_G \rho_G \bar{v}_G \frac{\partial \bar{v}_G}{\partial \chi} + \varepsilon_G \frac{\partial P_i}{\partial \chi} - \frac{F}{\xi_i}\varepsilon_G \rho_G g$$

$$\frac{\partial \varepsilon_G}{\partial \chi} = \left|\tau_{wG}\right| \frac{\xi_{wG}}{F} + \tau_i \frac{\xi_i}{F} \tag{7}$$

and

$$\varepsilon_L \rho_L \bar{v}_L \frac{\partial \bar{v}_L}{\partial \chi} + \varepsilon_L \frac{\partial P_i}{\partial \chi} + \frac{F}{\xi_i}$$
$$\varepsilon_L \rho_L g \frac{\partial \varepsilon_L}{\partial \chi} = -\left|\tau_{wL}\right| \frac{\xi_{wL}}{F} - \frac{\tau_i \xi_i}{F} \tag{8}$$

Eliminating the pressure gradient in Eq. (7) and Eq. (8) and then using the equation for

conservation of mass and the relation $\varepsilon_G + \varepsilon_L = 1$, the following equation is obtained.

$$\rho_G \bar{v}_G \left[\frac{-\bar{v}_G}{\varepsilon_G} \frac{\partial \varepsilon_G}{\partial \chi} \right] - \rho_L \bar{v}_L \left[\frac{\bar{v}_L}{\varepsilon_L} \frac{\partial \varepsilon_G}{\partial \chi} \right] + (\rho_L - \rho_G) \frac{F_G}{\xi_i} \frac{\partial \varepsilon_G}{\partial \chi}$$

$$= \left| \tau_{wG} \right| \frac{\xi_{wG}}{F\varepsilon_G} - \left| \tau_{wL} \right| \frac{\xi_{wL}}{F\varepsilon_L} + \frac{\tau_i \xi_i}{F\varepsilon_G} + \frac{\tau_i \xi_i}{F\varepsilon_L} \quad (9)$$

and then

$$\frac{\partial \varepsilon_G}{\partial \chi} = \frac{4}{\pi D^2} \frac{\left[\frac{\left| \tau_{wG} \right| \xi_{wG}}{\varepsilon_G} + \frac{\left| \tau_{wL} \right| \xi_{wL}}{\varepsilon_L} + \frac{\tau_i \xi_i}{\varepsilon_G} + \frac{\tau_i \xi_i}{\varepsilon_L} \right]}{\left[\frac{(\rho_L - \rho_G) Fg}{\xi_i} - \frac{\rho_L \bar{v}_L^2}{\varepsilon_L} - \frac{\rho_G \bar{v}_G^2}{\varepsilon_G} \right]} \quad (10)$$

Recalling the definition of the dimensionless superficial velocity of phase k

$$j^*_k = j_k \left[\frac{\rho_k}{(\rho_L - \rho_G) gD} \right]^{1/2} \quad (11)$$

(k : L = Liquid, G = Gas)

where j_k is the superficial velocity and defined by $j_k = \varepsilon_k \bar{v}_k$.

j^*_k is also called dimensionless densimetric Froude number or the Wallis parameter which has been proposed as one of the typical parameters for CCFL studies.

It is easy to show that Eq. (10) may be written as

$$D \frac{\partial \varepsilon_G}{\partial \chi} = \frac{\frac{4\varepsilon_L \varepsilon_G}{(\rho_L - \rho_G) g\pi D^2}}{\left[\frac{\left| \tau_{wG} \right| \xi_{wG}}{\varepsilon_G} + \frac{\left| \tau_{wL} \right| \xi_{wL}}{\varepsilon_L} + \frac{\tau_i \xi_i}{\varepsilon_G \varepsilon_L} \right]} - \frac{\pi D \varepsilon_G \varepsilon_L}{4\xi_i} - \frac{\varepsilon_L (j_G^*)^2}{\varepsilon_G^2} - \frac{\varepsilon_G (j_L^*)^2}{\varepsilon_L^2} \quad (12)$$

The wall momentum transfer term is expressed as

$$\tau_{wk} = (-1)^a \frac{1}{2} \psi_{wk} \rho_k \bar{v}_k^2 \quad (13)$$

where a = 1 for k = G and a = 2 for k = L

and with $\tau_{wG} = \tau_i$

$$\psi_{wG} = C_G Re_G^{-n}, \quad \psi_{wL} = C_L Re_L^{-m} \quad (14)$$

where Reynald number of phase k is defined by

$$Re_k = \frac{\rho_k \bar{v}_k D_{kh}}{\mu_k} \quad (15)$$

The hydraulic diameter D_{kh} is defined by Agrawal et al. [5] as follows :

$$D_{Gh} = \frac{4 F_G}{(\xi_{wG} + \xi_i)}$$

and

$$D_{Lh} = \frac{4 F_L}{\xi_{wL}} \quad (16)$$

For turbulent flow C_k = 0.046, n = m = 0.2; for laminar flow C_k = 16, n = m = 1.

For free outfall at the horizontal outlet section, this mathematical form can be expressed as

$$\frac{\partial \varepsilon_G}{\partial \chi} \longrightarrow \infty \quad (17)$$

It can be shown from Eq. (12) that under the condition of Eq. (17), it satisfies that

$$\frac{(j^*_G)^2}{\varepsilon^3_G} + \frac{(j^*_L)^2}{\varepsilon^3_L} = \frac{\pi D}{4\xi_i} \qquad (18)$$

Gardner [6] has got the same equation from his derivation. This equation represents the condition for the transition to supercritical flow where any small interfacial disturbance will be held stationary and cannot propagate against the flow[11]. The equation recognise as the equation for two-phase critical flow. For an open channel flow (i.e. without the influance of the gas flow) the above condition reduces to the form of

$$\frac{(j^*_L)^2}{\varepsilon^3_L} = \frac{\pi D}{4\xi_i} \qquad (19)$$

This equation is the classical equation for critical flow in open channel.

If the right side of the Eq. (12) represent by α.

It can be simplified as

$$\frac{d\chi}{D} = \frac{d\varepsilon_G}{\alpha} \qquad (20)$$

Eq. (20) can be integrated from the location of the hydraulic jump (at which void fraction is $\varepsilon_{G,C}$) to the point where the critical flow occurs (at which void fraction is $\varepsilon_{G,e}$). The distance between these is nominally taken to be the length of the horizontal section L. Thus we have

$$\frac{L}{D} = \int_{\varepsilon_{G,c}}^{\varepsilon_{G_e}} \frac{d\varepsilon_G}{\alpha} \qquad (21)$$

Eq. (21) will be solved iteratively for j^*_G and j^*_L with $\varepsilon_{G,e}$ determined from Eq. (18) and $\varepsilon_{G,c}$ determined from $j^*_G = 0.82\ \varepsilon_G^{2.75}$ which is the experimental correlation as described in the Part I. [10] The solution is a pair of dimensionless superficial velocity which, for the particular choice of pipe geometry, defines the flooding point.

FLOODING CURVES FROM CALCULATIONS

The results from the calculation using the method described above are shown in *Figure 3*. It shows the diffferent flooding curves which are produced from the calculations at different length to diameter ratios. Air and water are used as working fluids. The wall momentum transfer terms are calculated based on $n = m = 0.2$, $C_G = C_L = 0.046$ for turbulent flow and $n = m = 1$, $C_G = C_L = 16$ for laminar flow. The phase Reynolds number are evaluated from hydraulic diameter as suggested by Agrawal et al. [5]. It is interesting to consider that the interface momentum transfer term is taken as equal to the wall momentum transfer term in the part of the pipe occupied by the gas phase. This same assumption was used for the work of Gazley [7], Taitel et al. [2], and Ardron et al. [4]. With this method, the flooding curves for various combination of working fluids, for example, steam and water can also be produced. However, the suitable fluid properties and interfacial friction factor are needed.

COMPARISON WITH EXPERIMENTAL DATA

Figures 4 and 5 show comparisons of the air-water results obtained from experimental data with those predicted by present model. The agreement of the present model to the experimental data is satisfactory especially for large length to diameter ratios. The reason is probably due to using the assumption that the critical flow condition occurs at the pipe exit, E. In real situation for circular pipe, due to the two dimensional effect, the critical flow condition occurs about one or two diameter upstream. In case of pipe with large length to diameter ratio, the error from two-dimensional effects is dominated. That is reason why at

large length to diameter ratio, the experimental data agree quite well with the model. However, for greater liquid flow rates, their predictions fail due to change in the flooding mechanism. For very high liquid flow rate, the liquid flow remains supercritical in the horizontal part and the model is not applicable to this situation. The model also gives the liquid zero penetration limit ($j^*_L = 0$) correspond to the experimental data.

The data obtained by Wan et al [8] and Siddique et al. [9] are compared with the predictions of the present model. *Figures 6 and 7* show those comparisons with air-water as working fluid. Reasonable agreement between the model and the experiment is obtained for $j^{*}_{L}{}^{1/2} < 0.5$. Above this limit, the mechanism of flooding is different, flooding occurs as a result of slug formation far away from the bend.

CONCLUSION

An analytical model for two Phase flow is developed for predicting the countercurrent flow limitation (or the onset of flooding) for a horizontal pipe with bend. The model development is based on visual observation that liquid entering the bend formed the hydraulic jump close to the bend in the horizontal part. The flow conditions between the hydraulic jump and critical outflow of water are determined by solving the two-fluid mass and momentum conservations for steady horizontal stratified countercurrent flow. An empirical correlation which is the relation between dimensionless superficial gas velocity and the void fraction at onset of flooding near the bend is used in the mathematical model. The results from the model are compared with the present experimental data and the data obtained by other researchers. The agreement between the theory and the experimental results is satisfactory as a function of the length to diameter ratio. The model can predict the onset of flooding at specific interval of liquid flow rate which the flooding coincides with slugging at the crest of hydraulic jump near the bend. (or in the first region of flooding curve)

ACKNOWLEDGEMENT

The author thanks the Thailand Research Fund (TRF) for encouragement to continue this work.

REFERENCES

1. Bankoff, S.G. and Lee, S.C., A Review of Countercurrent Flooding Models Applicable to PWR Geometries, Nuclear Safety, 26 (2), March-April 1985.

2. Taitel, Y., Dukler, A.E., A Model for Predicting Flow Regime Transitions in Horizontal and Near-Horizontal Gas-Liquid Flow, AlChE J. 22 (1), 47-55, 1976.

3. Wongwises, S. Experimental Investigation of Two-Phase Countercurrent Flow Limitation in a Bend between Horizontal and Inclined Pipes, Int. J. Exp. Thermal & Fluid Sci., 8 (3), 245-259, 1994.

4. Ardron, K.H., Banerjee, S, Flooding in an Elbow Between a Vertical and a Horizontal or Near Horizontal Pipe; Int. J. Multiphase Flow 12 (1), 543-558, 1986.

5. Agrawal S.S., Gregory, G.A., Govier, G.W., An analysis of Horizontal Stratified Two-Phase Flow in Pipes, Can. J. Chem. Eng. 51, 280-286, 1973.

6. Gardner, G.C., Co-current Flow of Air and Water From a Reservior into a Short Horizontal Pipe, Int. J. Multiphase Flow, 14 (4), 375-388, 1988.

7. Gazley, C., Interfacial Shear and Stability in Two-Phase Flow. Ph.D. Thesis,

University of Delaware, 1949.

8. Wan, P.T., Krishnan, V.S., Air-Water Flooding in a 90° Elbow With a Slightly Inclined Lower Leg, Proc. CNS 7th Annual Conference, Toronto, June 1986.

9. Siddiqui, H., Banerjee, S., Ardron, K.H., Flooding in an Elbow Between a Vertical and a Horizontal or Near-horizontal pipe.; Int. J. Multiphase Flow 12 (1) 531-541, 1986.

10. Wongwises, S., Countercurrent Flooding in a Horizontal Pipe with Bend, Part I : Experiment, R & D Journal of EIT, 5 (2), 1994.

11. Choi K.Y., NO H.C., Experimental Studies of Flooding in Nearly Horizontal Pipes, Int. J. Multiphase Flow 21 (3) 419-436, 1995.

NOMENCLATURE

C_G	parameter defined in eq. (14)
C_L	parameter defined in eq. (14)
D	pipe diameter, m
F	crossectional area of pipe, m^2
g	gravitational acceleration, m/s^2
L	pipe length, m
m	parameter defined in eq. (14)
n	parameter defined in eq. (14)
p	pressure, Pa
$\overline{P}$	average pressure, Pa
ΔP	pressure drop, Pa
j	superficial velocity, m/s
$\overline{v}$	average velocity, m/s
j^*	dimensionless superficial velocity defined by eq. (11)

Greek Symbols

μ	dynamic viscosity, Pa.sec
γ	kinematic viscosity, m^2/sec
ε_L	liquid hold-up, dimensionless
ε_G	void fraction, dimensionless
θ	inclination angle of bend, degree
ρ	density, kg/m^3
β	angle defined in figure 2
ξ	perimeter, m
τ	shear stress, N/m^2
α	the right side term of eq.(12)

Subscripts

k	gas or liquid
i	interface or inlet
o	outlet
G	gas
L	liquid
wG	wall-gas
wL	wall-liquid
kh	hydraulic value of phase k

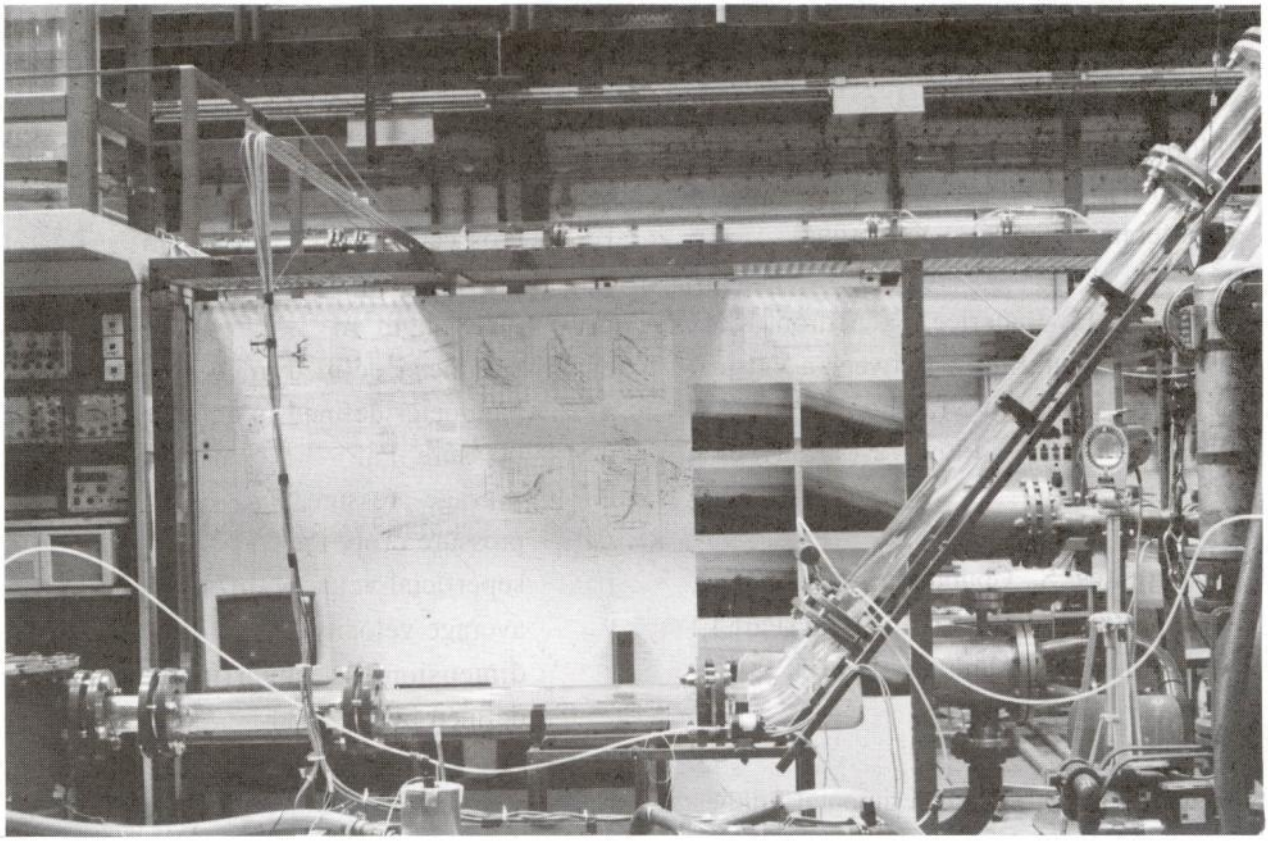

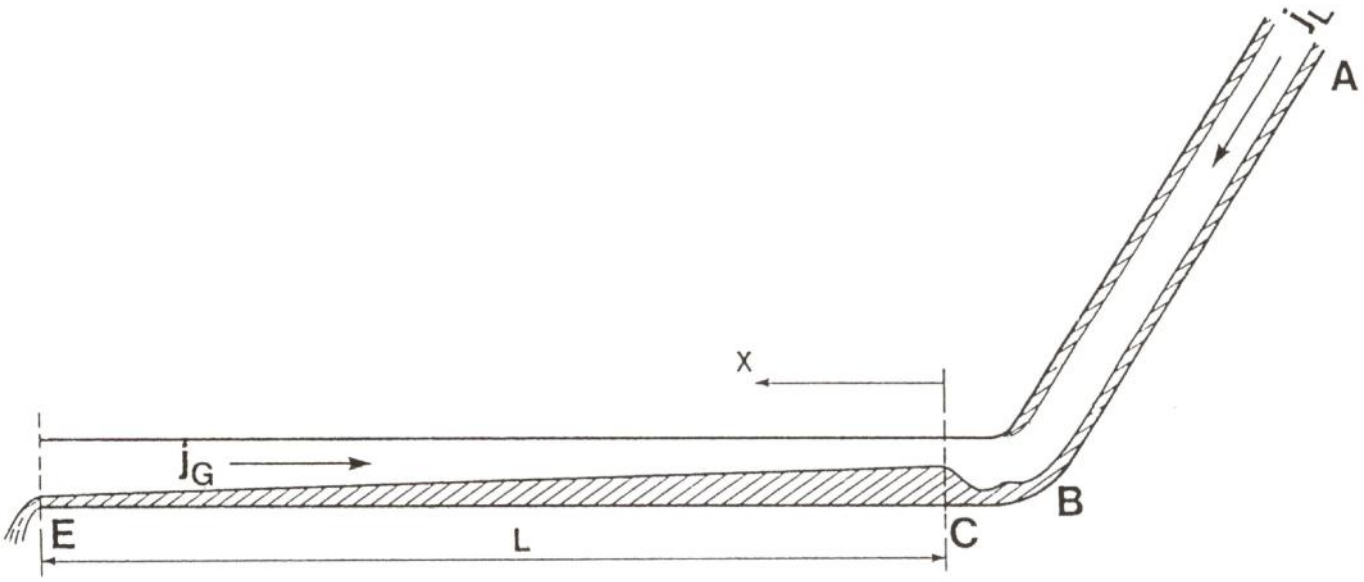

Figure 1: Model for countercurrent two-phase flow during flooding in a horizontal pipe with bend

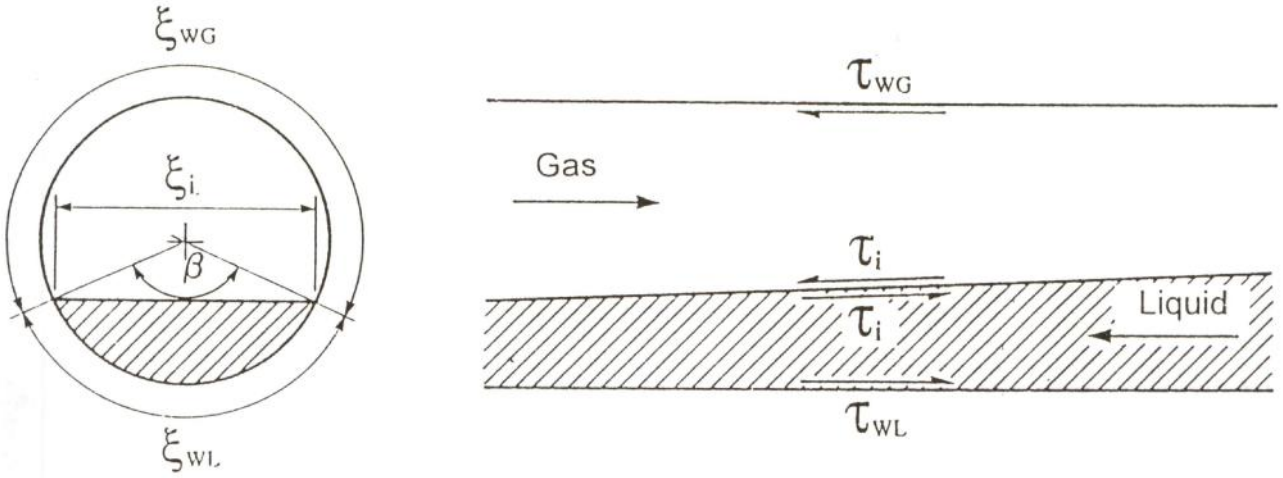

Figure 2: Stratified countercurrent flow

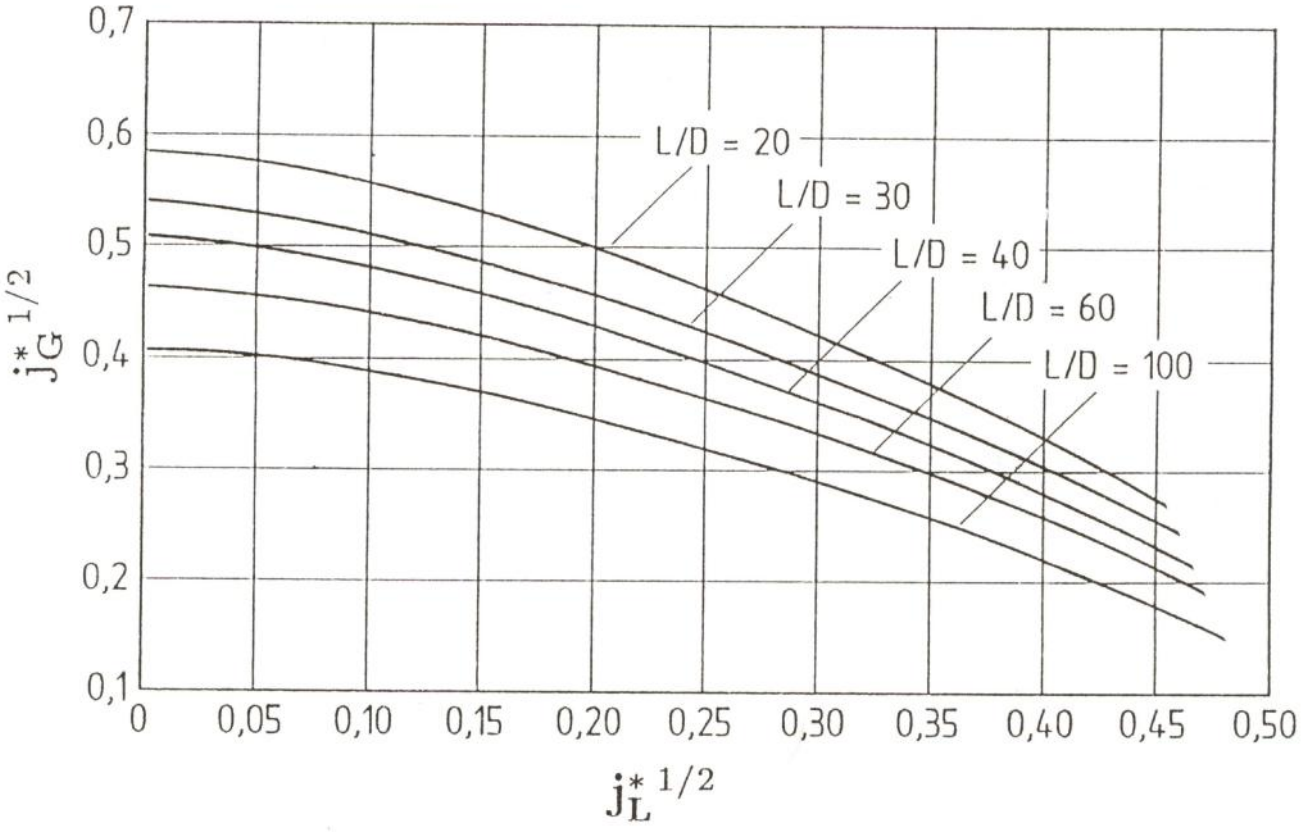

Figure 3: Predicted flooding curves

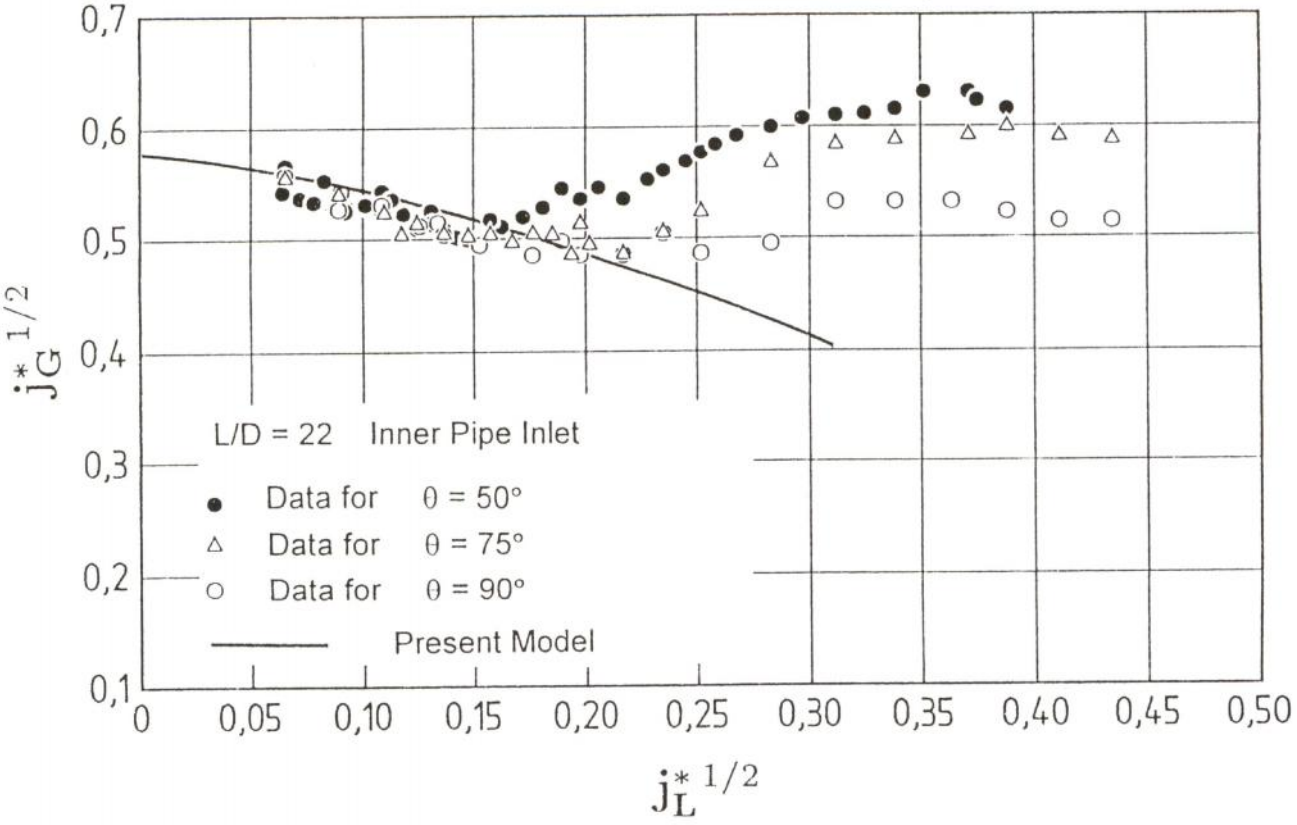

Figure 4: Comparison of experimental data with the predictions

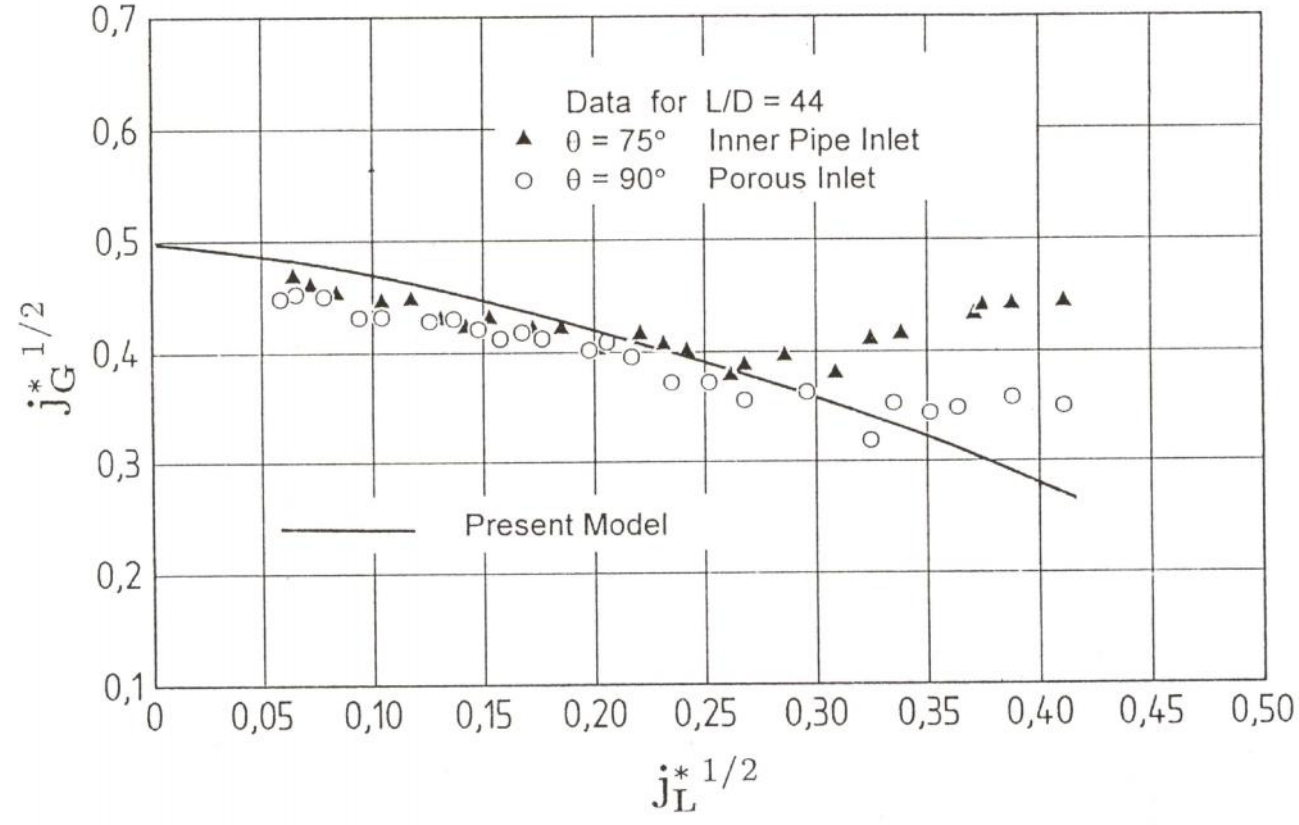

Figure 5: Comparison of experimental data with the predictions

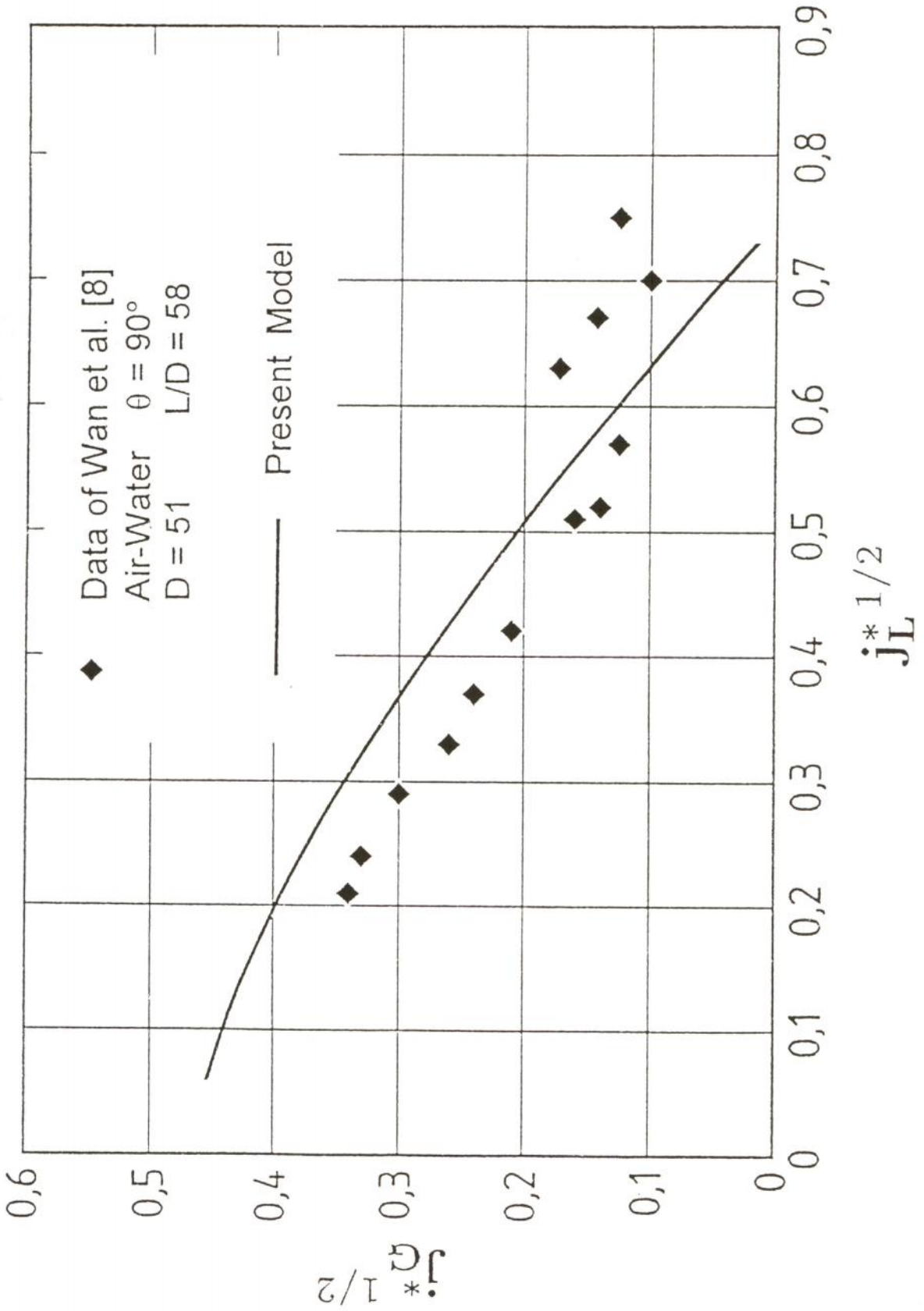

Figure 6: Comparison of air-water flooding data of Wan et al. [8] with the predictions

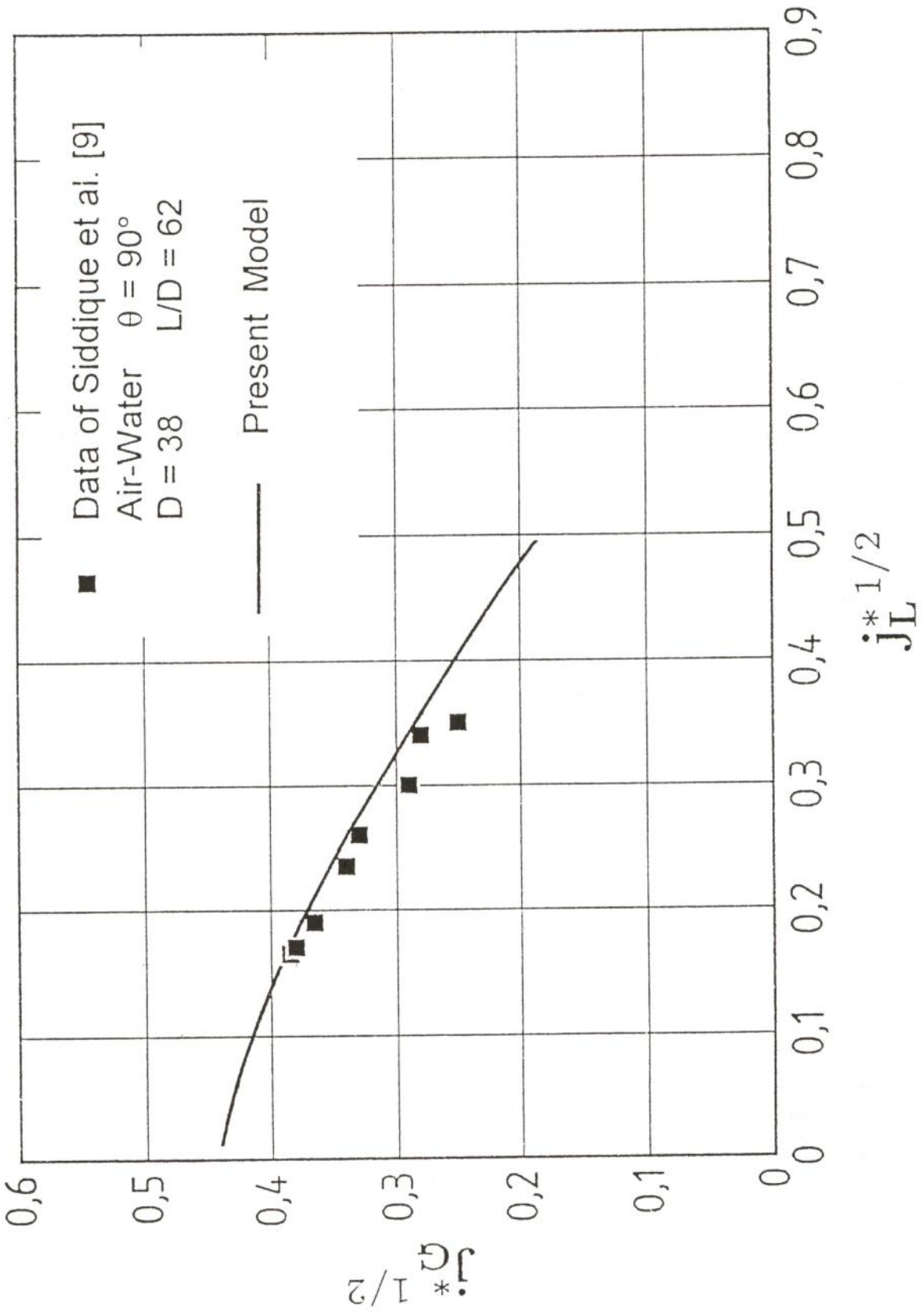

Figure 7: Comparison of air-water flooding data of Siddique et al. [9] with the predictions